



Establishment of Rapid and Accurate Screening System for Molecular Target Therapy of Osteosarcoma

Technology in Cancer Research & Treatment
Volume 21: 1-9
© The Author(s) 2022
Article reuse guidelines:
sagepub.com/journals-permissions
DOI: 10.1177/15330338221138217
journals.sagepub.com/home/tct


Keita Sasa, MD^{1,2}, Tsuyoshi Saito, MD, PhD^{2,3} , Taisei Kurihara, MD, PhD¹, Nobuhiko Hasegawa, MD, PhD¹, Kei Sano, MD, PhD¹, Daisuke Kubota, MD, PhD¹, Keisuke Akaike, MD, PhD¹, Taketo Okubo, MD, PhD¹, Takuo Hayashi, MD, PhD², Tatsuya Takagi, MD, PhD¹, Muneaki Ishijima, MD, PhD¹, and Yoshiyuki Suehara, MD, PhD^{1,3}

Abstract

Introduction Comprehensive analyses using clinical sequences subcategorized osteosarcoma (OS) into several groups according to the activated signaling pathways. Mutually exclusive co-occurrences of gene amplification (*PDGFRA/KIT/KDR*, *VEGFA/CCND3*, and *MDM2/CDK4*) have been identified in approximately 40% of OS, representing candidate subsets for clinical evaluation of additional therapeutic options. Thus, it would be desirable to evaluate the specific gene amplification before starting therapy in patients with OS. **Materials and Methods** This is a retrospective study. We examined 13 cases of clinical OS samples using NanoString-based copy number variation (CNV) analysis. Decalcification and chemotherapeutic effects on this analysis were also assessed. **Results** First, the accuracy of this system was validated by showing that amplification/deletion data obtained from this system using various types of cancer cell lines almost perfectly matched to that from the Cancer Cell Line Encyclopedia (CCLE). We identified potentially actionable alterations in *CDK4/MDM2* amplification in 10% of samples and potential additional therapeutic targets (*PDGFRA/KIT/KDR* and *VEGFA/CCND3*) in 20% of samples, which is consistent with the reported frequencies. Furthermore, this assay could identify these potential therapeutic targets regardless of the sample status (frozen vs formalin-fixed paraffin-embedded [FFPE] tissues). **Conclusion** We established a NanoString-based rapid and cost-effective method with a short turnaround time (TAT) to examine gene amplification status in OS. This CNV analysis using FFPE samples is recommended where the histological evaluation of viable tumor cells is possible, especially for tumors after chemotherapy with higher chemotherapeutic effects.

Keywords

osteosarcoma, molecular target therapy, gene amplification, NanoString, rapid screening, chemotherapy

Abbreviations

CCLE, Cancer Cell Line Encyclopedia; CNV, copy number variation; FISH, fluorescence in situ hybridization; FFPE, formalin-fixed paraffin-embedded; ICIs, immune checkpoint inhibitors; IHC, immunohistochemistry; NGS, next-generation sequencing; OS, osteosarcoma; SD, standard deviation; TAT, turnaround time; WES, whole exome sequencing

Received: May 4, 2022; Revised: October 2, 2022; Accepted: October 17, 2022.

¹ Department of Medicine for Orthopaedics and Motor Organ, Juntendo University School of Medicine, Tokyo, Japan

² Department of Human Pathology, Juntendo University School of Medicine, Tokyo, Japan

³ Intractable Disease Research Center, Juntendo University, Graduate School of Medicine, Tokyo, Japan

Corresponding Authors:

Tsuyoshi Saito, Department of Human Pathology, MD, PhD, Department of Medicine for Orthopaedics and Motor Organ, Juntendo University School of Medicine, Tokyo, 113-8421, Japan.

Email: tysaitou@juntendo.ac.jp

Yoshiyuki Suehara, MD, PhD, Intractable Disease Research Center, Juntendo University, Graduate School of Medicine, Tokyo, 113-8421, Japan.

Email: ysuehara@juntendo.ac.jp



Introduction

Osteosarcoma (OS) is the most common primary malignant bone tumor. OS most commonly arises in the metaphysis of the long bones near the growth plates, with two-thirds of tumors emerging around the knee joint in the distal femur, followed by the proximal tibia as the second most frequent site. More than 85% of patients present with localized diseases. The standard protocol for the treatment of patients with OS was established more than 30 years ago (chemotherapy and surgical resection), and limited therapeutic progress has been made since that time. The treatment results of the advanced cases at the first visit were still extremely poor. It is possible that new anticancer drugs have not emerged partly due to the limited number of chemotherapeutic agents. Novel antibody-based therapies such as HERCEPTIN and immunotherapy with immune checkpoint inhibitors (ICIs) have also been introduced, although they have not drastically improved the survival of patients with OS.

Recently, next-generation sequencing (NGS)-based research has opened the possibility of new molecular target therapies for OS.¹⁻⁴ Our group and others conducted a comprehensive analysis using clinical sequences such as MSK-IMPACT and subcategorized OS into several groups according to the activated signaling pathways. Some of the activated pathways/amplified genes were reproducible across the studies. In addition, mutually exclusive co-occurrence of gene amplification was identified in approximately 40% of OS cases, representing candidate subsets for clinical evaluation of additional therapeutic options.

Therefore, it would be desirable to evaluate specific gene amplifications before starting therapy in patients with OS. However, the cost of NGS is generally high, and formalin fixation can cause DNA fragmentation, degradation, cross-linking, and adduct formation, which can theoretically impact molecular studies.⁵ In addition, along with the age of the sample, DNA from bone tumors usually undergoes severe nucleic acid degradation during the decalcification process.² Thus, formalin-fixed paraffin-embedded (FFPE) samples are generally not suitable for NGS analysis. We aimed to establish a simple and cost-effective method to examine gene amplification status in OS using NanoString.

Materials and Methods

Cell Lines

Nine cell lines (5 OS cell lines, MG63, KHOS, 143 B, U2OS, and G292 and 4 other cancer cell lines from different organs, U251MG, HCC1569, NCI-H146, and HPAF-II) were maintained in a 37 °C incubator with 5% CO₂ in a humidified atmosphere. These cell lines were grown in DMEM or RPMI with 10% FBS, 100 mg/mL penicillin, and 100 mg/mL streptomycin. The cells were harvested at 80% confluence. Genomic DNA was extracted from each cell line using a DNA extraction kit (QIAamp DNA Mini Kit). Furthermore, these cell lines

harvested at the same point were fixed with 10% buffered formalin (12 h) and embedded in paraffin to reproduce the FFPE process during routine histopathological diagnosis. Genomic DNA was also extracted from these FFPE cell lines using a DNA extraction kit (QIAamp DNA FFPE Tissue Kit). Samples were treated with RNase A (Qiagen, Hilden, Germany) according to the manufacturer's protocol.

Clinical Samples

Thirteen frozen OS samples were collected at the Department of Medicine for Orthopaedics and Motor Organ, Juntendo University Hospital. Genomic DNA was extracted from tumoral and corresponding nontumoral tissues using the QIAamp DNA Mini Kit or QIAamp DNA FFPE Tissue Kit according to the manufacturer's protocols. Samples were treated with RNase A, according to the manufacturer's protocol. DNA concentration and 260/280 and 260/230 nm ratios were measured using Nanodrop. Eight cases were osteoblastic OS, 2 were extraskeletal OS, and there was 1 case each of chondroblastic OS, periosteal OS, and secondary OS arising from giant cell tumors of the bone. Frozen samples from 3 patients were obtained after chemotherapy, whereas the remaining 10 patients did not receive chemotherapy. The chemotherapeutic effects of these 3 patients were grades 1, 3, and 4, respectively. Neither of the patients with extraskeletal OS received chemotherapy. Tumoral and corresponding nontumoral DNA was extracted from 10 out of 13 cases of FFPE where available. Three cases were excluded from this analysis due to the absence of nonnormal tissues or because the preoperative biopsy samples were too small to be analyzed. Five out of 13 FFPE samples (Cases# 1, 2, 6, 9, and 11) were analyzed using TruSight™ Tumor170 (Illumina), and the copy number variation (CNV) data were compared to those analyzed by NanoString. The cut-off for amplification was defined as 2.0.

NanoString-Based CNV Analysis

NanoString-based CNV analysis was performed using nCounter (NanoString Technologies).^{6,7} To elucidate the co-amplification status of genes previously reported to occur in a mutually exclusive manner (*PDGFRA/KIT/KDR*, *VEGFA/CCND3*, *MDM2/CDK4*, *MYC*, and so on; 24 genes total) in OS,¹ we created a custom probe set in the NanoString assay. The probe list used in this assay is described in Supplementary Table 1. Three probes were prepared for each gene. For cell lines, CNV data analysis was performed as follows: Each data set was normalized by dividing them by the corresponding U2OS scores, which are shown to only have *MYC* amplification among genes included in this gene set. Three normalized scores of each gene were added and the mean values and standard deviation (SD) were calculated. Amplification/deletion information of each cell line was obtained from the Cancer Cell Line Encyclopedia (CCLE). For clinical samples, each data point was normalized as follows: each score from the tumoral DNA was divided by

the score from the corresponding nontumoral DNA, and 3 normalized scores of each gene were added, with the mean values then calculated. Nine cell lines (prepared as fresh and FFPE samples), 13 clinical frozen samples of OS, and corresponding 8 decalcified/2 nondecalified FFPE samples were used as samples. Three FFPE samples were excluded due to inadequate sample sizes for analysis. Genomic DNA was extracted from each sample using the Qiagen kit (QIAamp DNA Mini Kit and QIAamp DNA FFPE Tissue Kit). According to the sample status, 150 to 300ng of DNA was processed for the NanoString nCounter copy number variant analysis according to the manufacturer's protocol (NanoString Technologies). Briefly, 150 to 300ng of genomic DNA was fragmented by Alul-based fragmentation and hybridized to the probes (a reporter probe and a capture probe) at 65 °C for 18 to 24 h using a thermal cycler. Samples were added into the nCounter Prep Station for 3 h to remove excess probes, purify, and immobilize the sample on the internal surface of the cartridge. Finally, the sample cartridge was transferred to the nCounter Digital Analyzer, where color codes were counted and tabulated for each target molecule. The expression number for the base sequence of the probe part was analyzed using nSolver Analysis Software Version 4.0 (<https://www.nanostring.com/products/analysis-software/nsolver>). All experiments were performed in a single run without any replicate, although 3 probes are designed for each gene and 3 normalized scores of each gene were added and then mean values and SD were calculated to compare data in each group. The methodology of this system is also described in the NanoString HP (nCounter® Gene Fusion Panels and CNV Assays | NanoString).

Statistical Analysis

Mann–Whitney test was performed using 3 values obtained from 3 each probe to evaluate the statistical difference between the 2 groups. *P*-value < .05 was considered as statistically significant.

Ethical Standards

This is a retrospective study. This study was reviewed and approved by the Juntendo University School of Medicine (Tokyo, Japan) Institutional Review Board (#21-079, approved on July 6, 2021). This study was a cross-sectional study and does not contain in vivo data. We have obtained written informed consent from the patient to analyze tumor specimens and normal tissue.

Results

Cell Lines

The obtained gene amplification status by NanoString analysis was concordant with that described in the CCLE cell line database (Table 1, Supplementary Figure S1). The amplification status of *MYC* in U2OS was not directly assessed; however, the relative score of *MYC* in U2OS was almost similar to that

in HCC1569 and G292, which were described to have *MYC* amplification. These findings confirm the accuracy and quality of the custom probe set. Next, we assessed the effect of formalin fixation on this assay system. The same pattern of gene amplification was obtained between each DNA derived from the fresh cell line and the corresponding formalin-fixed cell line in all 9 of the cell lines. Thus, it was confirmed that sample fixation with formalin did not affect the results of this assay.

Clinical Samples

We analyzed 13 clinical OS samples (Table 2). Among the 10 cases without chemotherapeutic effects, one case showed potentially actionable alteration of *CDK4/MDM2* amplification (10%). Furthermore, *PDGFRA/KIT/KDR* amplification in 1 case and *CCND3/VEGFA* amplification in 1 case were identified as potential additional therapeutic targets (20%). However, 3 cases with pathological information of chemotherapeutic effects did not show amplification in these potentially actionable genes, although mild amplifications were observed in other genes such as *AKT1*, *AKT2*, *CCNE1*, and *NTRK1* (Supplementary Table 2).

Next, we analyzed the effect of decalcification during routine histopathological evaluation (Table 3 and Supplementary Table 3). Matched analysis between frozen and FFPE samples after decalcification was available for 6 cases (Cases #1, 2, 8, 10, 11, and 13), although the comparison was made based on the data from postchemotherapeutic samples in 2 cases (Cases #8 and 10). The obtained findings were concordant throughout the potentially actionable genes between frozen and FFPE samples in 5 out of 6 cases (83%). In the remaining case showing a higher chemotherapeutic effect (Case #10: grade 3), amplifications in *CCND3/VEGFA* and *CDK4/MDM2* were observed only in FFPE samples, although these differences were not statistically significant.

Furthermore, we evaluated the CNV changes affected by chemotherapy in 2 cases with the same sample status (Cases #1 and 2). Amplification status was enhanced in these 2 cases after chemotherapy (*CCND3/VEGFA* and *MYC/CDKN2A* in 2 cases), however, these differences were not statistically significant. In addition, the amplification status seemed to be different before and after chemotherapy in 2 cases (Cases #7 and 10), although the comparisons were made using different sample statuses (frozen vs FFPE) and the differences were not statistically significant. These 2 cases histologically showed higher chemotherapeutic effects, and frozen samples were taken from areas where the therapeutic effects were unknown, while the maximum viable tumor areas were selected from FFPE sections. Thus, the viable tumor content seemed to have influenced the different findings.

Discussion

The survival rate in OS has not drastically changed during the past 30 years, although subtle improvements have been noted

Table 1. Copy Number Variation (CNV) Analysis in Cell Lines.

	MG63	MG63-B	U251	U251-B	HCC1569	HCC1569-B	NCI-H146	NCI-H146-B	G292	G292-B	HPAF2	HPAF2-B	KHOS	KHOS-B	143B	143B-B	U2OS	U2OS-B
<i>PDGFRA</i>	2.71	2.63	2.89	3.10	0.85	0.82	1.13	1.08	0.70	0.62	0.59	0.49	0.66	0.68	1.03	1.09	1.00	1.00
±SD	0.20	0.21	0.40	0.17	0.06	0.14	0.23	0.07	0.05	0.03	0.07	0.01	0.03	0.14	0.04	0.22		
<i>P value</i>		.70	.70	.70	.70	.70	.70	.70	.20	.20	.10	.10	.70	.70	.70	.70		
<i>KIT</i>	0.39	0.42	1.49	1.44	0.74	0.73	0.85	0.84	0.61	0.61	0.50	0.47	0.54	0.56	0.86	0.87	1.00	1.00
±SD	0.02	0.01	0.03	0.06	0.02	0.05	0.01	0.04	0.02	0.03	0.03	0.06	0.01	0.01	0.01	0.03		
<i>P value</i>		.20	.40	.40	>.99	>.99	.70	.70	>.99	>.99	.70	.70	.10	.10	>.99	>.99		
<i>KDR</i>	0.39	0.42	1.53	1.52	0.75	0.72	0.84	0.83	0.61	0.60	0.51	0.47	0.58	0.57	0.88	0.91	1.00	1.00
±SD	0.00	0.04	0.07	0.02	0.02	0.05	0.06	0.03	0.01	0.01	0.02	0.07	0.02	0.04	0.03	0.06		
<i>P value</i>		.70	.70	.70	.80	.80	.60	.60	.50	.50	.70	.70	.70	.70	.70	.70		
<i>CCND3</i>	0.70	0.63	1.07	1.12	2.33	2.28	1.64	1.84	0.96	0.80	0.83	0.71	1.05	1.02	1.37	1.16	1.00	1.00
±SD	0.02	0.05	0.06	0.03	0.06	0.38	0.12	0.22	0.05	0.05	0.03	0.06	0.05	0.15	0.06	0.07		
<i>P value</i>		.10	.20	.20	>.99	>.99	.30	.30	.10	.10	.10	.10	>.99	>.99	.10	.10		
<i>VEGFA</i>	0.61	0.45	1.02	1.09	2.18	2.29	1.76	1.73	0.88	0.61	0.86	0.69	0.97	0.99	1.38	1.14	1.00	1.00
±SD	0.03	0.01	0.01	0.10	0.12	0.11	0.08	0.12	0.06	0.05	0.05	0.04	0.08	0.10	0.08	0.09		
<i>P value</i>		.10	.60	.60	.40	.40	.70	.70	.10	.10	.10	.10	.70	.70	.10	.10		
<i>CDK4</i>	0.93	0.81	0.64	0.66	0.98	0.92	0.99	0.99	12.36	10.22	1.63	1.42	0.94	0.89	1.03	0.89	1.00	1.00
±SD	0.05	0.05	0.03	0.02	0.05	0.06	0.10	0.07	0.12	0.97	0.12	0.14	0.04	0.03	0.15	0.01		
<i>P value</i>		.10	.70	.70	.30	.30	>.99	>.99	.10	.10	.20	.20	.30	.30	.60	.60		
<i>MDM2</i>	1.35	1.43	1.00	1.04	1.46	1.39	1.45	1.38	3.02	2.93	2.10	2.01	1.37	1.20	1.47	1.40	1.00	1.00
±SD	0.18	0.25	0.07	0.03	0.21	0.25	0.03	0.03	0.08	0.19	0.25	0.15	0.16	0.16	0.13	0.10		
<i>P value</i>		.70	.50	.50	>.99	>.99	.10	.10	.70	.70	.80	.80	.20	.20	>.99	>.99		
<i>MYC</i>	1.91	2.76	0.43	0.46	1.01	1.44	0.30	0.57	1.11	1.70	0.36	0.39	0.42	0.83	0.47	0.79	1.00	1.00
±SD	0.14	2.12	0.02	0.06	0.09	0.77	0.14	0.19	0.07	1.41	0.01	0.02	0.04	0.73	0.01	0.65		
<i>P value</i>		.70	.50	.50	.70	.70	.10	.10	.70	.70	.10	.10	>.99	>.99	.60	.60		
<i>CDKN2A</i>	0.01	0.01	0.02	0.02	1.44	1.48	1.78	1.93	0.69	0.67	1.19	1.37	0.01	0.01	0.01	0.01	1.00	1.00
±SD	0.01	0.01	0.01	0.01	0.14	0.16	0.13	0.19	0.08	0.02	0.18	0.24	0.01	0.01	0.01	0.01		
<i>P value</i>		>.99	>.99	>.99	>.99	>.99	.40	.40	>.99	>.99	.40	.40	>.99	>.99	.60	.60		

*-B: FFPE.

Table 2. Amplification Status of Therapeutic Candidate Genes in OS.

Case#	1	2	3	4	5	6	7	8	9	10	11	12	13
Diagnosis	Osteoblastic OS	Osteoblastic OS	Osteoblastic OS	Osteoblastic OS	Osteoblastic OS	Osteoblastic OS	Osteoblastic OS	Chondro. OS	Periosteal OS	from GCTB	Extraskelatal OS	Osteoblastic OS	Extraskelatal OS
Materials	Frozen Before CT	Frozen Before CT	Frozen Before CT	Frozen Before CT	Frozen Before CT	Frozen Before CT	Frozen After CT	Frozen After CT	Frozen Before CT	Frozen After CT	Frozen CT not performed	Frozen Before CT	Frozen CT not performed
Sample status													
Chemotherapeutic grade				4			4	1		3			
NGS data (FPPE)	<i>CCND3</i> <i>AMP</i> (after CT)	None (after CT)	N.D.	N.D.	N.D.	<i>MYC AMP</i> (before CT)	N.D.	N.D.	<i>MYC AMP</i> (before CT)	N.D.	<i>MYC, CCNE1 AMP</i> (before CT)	N.D.	N.D.
<i>PDGFRA</i>	1.22	2.81	0.65	1.21	1.04	0.96	0.93	1.04	0.97	1.06	1.13	1.17	0.77
<i>KIT</i>	1.27	2.43	0.63	1.45	1.09	1.13	1.02	0.79	1.03	1.00	1.26	1.08	0.70
<i>KDR</i>	1.19	2.28	0.62	1.43	1.04	1.06	1.01	0.95	1.03	0.98	1.16	1.12	0.69
<i>CCND3</i>	3.22	1.41	0.88	0.65	0.99	1.10	0.93	0.93	0.91	1.12	1.48	1.50	1.61
<i>VEGFA</i>	3.46	1.52	0.87	0.62	0.91	1.11	0.86	0.64	0.89	1.05	1.40	1.36	1.70
<i>CDK4</i>	1.06	1.17	0.66	0.64	1.00	0.70	0.83	0.65	0.91	1.11	1.08	8.40	0.91
<i>MDM2</i>	1.14	0.90	0.60	0.69	1.17	1.02	0.91	0.84	0.90	1.08	1.03	39.25	1.04
<i>MYC</i>	1.54	1.10	0.85	0.80	1.24	2.79	0.87	0.64	0.93	1.11	2.21	1.62	1.17
<i>CDKN2A</i>	0.76	0.98	0.93	0.49	1.02	0.67	0.90	0.65	1.00	1.02	1.57	0.88	1.57

Abbreviations: CT, chemotherapy; FPPE, formalin-fixed paraffin-embedded; GCTB, giant cell tumor of bone; N.D., not done; NGS, next-generation sequencing; OS, osteosarcoma.

Table 3. Comparison Between Frozen and FFPE Samples.

Case#	1 ^b		2 ^b		7		8		9		10		11		12		13						
	Osteoblastic OS		Osteoblastic OS		Osteoblastic OS		Chondroblastic OS		Periosteal OS		Extraskel OS		Osteoblastic OS		Extraskel OS		Extraskel OS						
Diagnosis	Frozen Before CT	FFPE After CT	Frozen Before CT	FFPE After CT	Frozen Before CT	FFPE After CT	Frozen Before CT	FFPE After CT	Frozen Before CT	FFPE After CT	Frozen Before CT	FFPE After CT	Frozen Before CT	FFPE After CT	Frozen Before CT	FFPE After CT	Frozen Before CT	FFPE After CT					
Materials Sample status	Grade 1	Grade 1	Grade 1	Grade 1	Grade 1	Grade 1	Grade 1	Grade 1	Grade 1	Grade 1	Grade 1	Grade 1	Grade 1	Grade 1	Grade 1	Grade 1	Grade 1	Grade 1					
Chemotherapeutic effect	None	None	None	None	None	None	None	None	None	None	None	None	None	None	None	None	None	None					
NGS (TruSight170) ^a	CCND3	CCND3	CCND3	CCND3	CCND3	CCND3	CCND3	CCND3	CCND3	CCND3	CCND3	CCND3	CCND3	CCND3	CCND3	CCND3	CCND3	CCND3					
	AMP (after chemo)	AMP (after chemo)	AMP (after chemo)	AMP (after chemo)	AMP (after chemo)	AMP (after chemo)	AMP (after chemo)	AMP (after chemo)	AMP (after chemo)	AMP (after chemo)	AMP (after chemo)	AMP (after chemo)	AMP (after chemo)	AMP (after chemo)	AMP (after chemo)	AMP (after chemo)	AMP (after chemo)	AMP (after chemo)					
	MYC	MYC	MYC	MYC	MYC	MYC	MYC	MYC	MYC	MYC	MYC	MYC	MYC	MYC	MYC	MYC	MYC	MYC					
	CCNE1	CCNE1	CCNE1	CCNE1	CCNE1	CCNE1	CCNE1	CCNE1	CCNE1	CCNE1	CCNE1	CCNE1	CCNE1	CCNE1	CCNE1	CCNE1	CCNE1	CCNE1					
	AMP (before chemo)	AMP (before chemo)	AMP (before chemo)	AMP (before chemo)	AMP (before chemo)	AMP (before chemo)	AMP (before chemo)	AMP (before chemo)	AMP (before chemo)	AMP (before chemo)	AMP (before chemo)	AMP (before chemo)	AMP (before chemo)	AMP (before chemo)	AMP (before chemo)	AMP (before chemo)	AMP (before chemo)	AMP (before chemo)					
<i>PDGFRA</i>	1.22	1.14	1.62	2.43	2.81	2.43	2.19	0.96	1.01	0.93	0.49	1.04	0.93	0.97	1.06	1.06	1.06	1.13	1.39	1.17	0.85	0.77	1.07
±SD	0.02	0.13	0.54	0.23	0.18	0.23	0.24	0.09	0.14	0.08	0.09	0.53	0.72	0.09	0.23	0.04	0.23	0.10	0.07	0.04	0.22	0.03	0.12
<i>P value</i>	.70	.20	.20	.10	.10	.10	.10	.10	.10	.10	.10	.70	.70	.10	.10	.10	.10	.10	.10	.10	.10	.10	.10
<i>KIT</i>	1.27	1.10	0.92	2.43	2.08	2.08	1.58	1.13	0.77	1.02	1.29	0.79	0.74	1.03	0.96	1.00	1.23	1.26	1.21	1.08	1.41	0.70	1.06
±SD	0.07	0.08	0.22	0.18	0.18	0.30	0.17	0.07	0.08	0.09	0.87	0.15	0.10	0.05	0.12	0.02	0.16	0.05	0.08	0.02	0.22	0.02	0.22
<i>P value</i>	.20	.40	.40	.40	.40	.70	.10	.10	.10	.70	.70	.10	.10	.70	.70	.10	.10	.10	.10	.10	.10	.10	.10
<i>KDR</i>	1.19	1.16	0.91	2.28	2.34	2.34	1.55	1.06	0.83	1.01	1.77	0.95	0.84	1.03	1.05	0.98	1.08	1.16	1.12	1.12	1.53	0.69	1.04
±SD	0.06	0.14	0.17	0.24	0.68	0.68	0.17	0.08	0.18	0.03	2.32	0.30	0.26	0.06	0.25	0.01	0.19	0.04	0.08	0.04	0.42	0.01	0.18
<i>P value</i>	.10	.10	.10	.10	.10	.10	.10	.10	.10	.10	.10	.10	.10	.10	.10	.10	.10	.10	.10	.10	.10	.10	.10
<i>CCND3</i>	3.22	3.26	6.28	1.41	1.17	1.52	1.10	1.19	0.93	0.93	1.99	0.93	0.79	0.91	1.30	1.12	5.58	1.48	1.59	1.50	1.18	1.61	1.03
±SD	0.64	0.61	3.38	0.07	0.18	0.37	0.08	0.20	0.11	1.28	0.08	0.26	0.26	0.04	0.16	0.06	2.27	0.08	0.12	0.06	0.28	0.04	0.18
<i>P value</i>	.10	.10	.10	.10	.10	.10	.10	.10	.10	.10	.10	.10	.10	.10	.10	.10	.10	.10	.10	.10	.10	.10	.10
<i>VEGFA</i>	3.46	2.70	7.92	1.52	1.14	1.14	2.39	1.11	0.74	0.86	11.16	0.64	0.45	0.89	0.83	1.05	2.66	1.40	1.61	1.36	0.87	1.70	1.06
±SD	0.16	0.29	2.36	0.04	0.25	0.41	0.01	0.17	0.04	10.33	0.13	0.16	0.16	0.02	0.08	0.02	0.14	0.05	0.40	0.12	0.08	0.10	0.14
<i>P value</i>	.10	.10	.10	.10	.10	.10	.10	.10	.10	.10	.10	.10	.10	.10	.10	.10	.10	.10	.10	.10	.10	.10	.10
<i>CDK4</i>	1.06	1.28	2.33	1.17	1.36	1.36	1.54	0.70	0.87	0.83	0.91	0.65	1.26	0.91	1.08	1.11	3.62	1.08	0.93	0.84	5.45	0.91	0.71
±SD	0.06	0.07	0.25	0.07	0.28	0.28	0.26	0.07	0.43	0.12	0.15	0.19	0.47	0.04	0.13	0.06	0.13	0.04	0.07	0.27	1.88	0.03	0.24
<i>P value</i>	.10	.10	.10	.10	.10	.10	.10	.10	.10	.10	.10	.10	.10	.10	.10	.10	.10	.10	.10	.10	.10	.10	.10
<i>MDM2</i>	1.14	1.11	1.44	0.90	0.84	0.84	0.94	1.02	0.88	0.91	0.69	0.84	1.65	0.90	0.98	1.08	2.24	1.03	1.07	39.25	30.36	1.04	1.23
±SD	0.04	0.03	0.45	0.03	0.11	0.14	0.09	0.22	0.03	0.15	0.22	0.69	0.69	0.06	0.22	0.03	0.38	0.05	0.11	3.32	15.45	0.01	0.45
<i>P value</i>	.40	.70	.70	.70	.70	.70	.40	.40	.40	.10	.10	.20	.20	.10	.10	.10	.10	.10	.10	.10	.70	.70	.70
<i>MYC</i>	1.54	1.47	4.17	1.10	0.96	1.10	2.03	2.79	1.46	0.87	1.97	0.64	1.30	0.93	1.69	1.11	1.07	2.21	4.56	1.62	1.39	1.17	1.20
±SD	0.09	0.16	2.18	0.08	0.27	0.90	0.03	0.40	0.01	1.45	0.14	0.67	0.67	0.03	0.34	0.02	0.44	0.10	0.24	0.23	0.54	0.03	0.55
<i>P value</i>	.70	.10	.10	.10	.10	.10	.10	.10	.10	.10	.10	.40	.40	.10	.10	.10	.10	.10	.10	.10	.10	.10	.10
<i>CDKN2A</i>	0.76	0.59	1.14	0.98	0.89	0.89	1.47	0.67	0.89	0.90	2.14	0.65	1.24	1.00	0.89	1.02	0.80	1.57	1.59	0.88	0.92	1.57	1.46
±SD	0.04	0.05	0.42	0.05	0.08	0.08	0.40	0.03	0.21	0.08	1.67	0.06	0.23	0.01	0.20	0.09	0.19	0.07	0.27	0.09	0.34	0.08	0.39
<i>P value</i>	.10	.10	.10	.10	.10	.10	.10	.10	.10	.10	.10	.10	.10	.10	.10	.10	.10	.10	.10	.10	.10	.10	.10
<i>RB1</i>	1.13	0.96	1.69	0.80	0.73	1.23	0.43	0.89	1.01	0.97	0.45	0.95	0.95	0.94	0.63	0.93	1.16	0.26	0.19	0.87	0.89	0.12	0.23
±SD	0.07	0.27	0.88	0.03	0.37	0.55	0.04	0.38	0.05	1.32	0.09	0.57	0.57	0.02	0.06	0.02	0.53	0.02	0.04	0.03	0.15	0.01	0.06
<i>P value</i>	.40	.40	.40	.40	.40	.40	.10	.10	.10	.10	.10	.10	.10	.10	.10	.10	.10	.10	.10	.10	.10	.10	.10

^aNGS data from Case#6 was obtained from FFPE biopsy sample before chemotherapy, however, the remaining biopsy sample was not adequate for this CNV analysis.

^bFor Case#1 and 2, statistical analysis was performed between frozen before CT and FFPE before CT samples, and between FFPE before CT and FFPE after CT samples.

Abbreviations: FFPE, formalin-fixed paraffin-embedded; NGS, next-generation sequencing; OS, osteosarcoma.

with changes in chemotherapeutic regimens.⁸ This is largely due to the lack of newly developed anticancer drugs. We have recently shown that approximately 20% of OS harbored potentially clinically actionable alterations based on the genomic sequencing data using MSK-IMPACT. We also showed that at least 40% of OS had amplifications (defined as 4 or more copies) of either *PDGFRA* located at 4q12 or *VEGFA* located at 6p12-21.¹ A recent study that analyzed the mutational profiles of pretreatment primary tumor samples from 33 OS patients using whole exome sequencing (WES) also showed that, when these 33 OS patients were divided into 2 groups according to clinical outcomes, 21 patients in the good prognosis group had tumor-free survival, whereas the remaining 12 patients in the poor prognosis group had lung metastases at initial diagnosis.⁹ Furthermore, they found significant differences in the number of somatic copy number alterations, including del (3p), amp (4q), del (7p), and amp (8q), between the 2 groups.⁹ Another study demonstrated that 6.4% of OS cases were enriched in 4q12 amplifications (defined as 6 or more copies) containing *PDGFRA/KIT/KDR*.¹⁰ In addition, it has also been reported that 6p12-21 amplification using NGS-based copy number assessment was confirmed in more than a fifth of all OS cases (24 of 111, 21.6%).¹¹ Although the frequency of patients with OS for clinical evaluation of these additional therapeutic options differs according to the criteria, the establishment of a simple screening system for CNV, especially of specific loci, is required.

NGS is very useful for comprehensively analyzing genetic alterations such as mutations, fusions, and amplifications/deletions; however, it is usually quite expensive and requires a relatively long turnaround time (TAT). Another method to evaluate the gene amplification status is fluorescence in situ hybridization (FISH), for example, *HER2* FISH, which is commonly used to evaluate therapeutic applications such as trastuzumab in breast cancer.¹²⁻¹⁶ Although its TAT is short, FISH targets only one gene status, and we cannot obtain further information even if the result is negative. Immunohistochemistry is an easy and cost-effective method with a short TAT that can be used to examine protein expression status and to test the application of molecular targeted therapies such as trastuzumab in breast cancer. Elevated *HER2* protein levels are shown to be tightly associated with gene amplification; thus, *HER2* protein levels can be semi-quantitatively assessed by immunohistochemistry (IHC), and the rates of concordance between IHC and FISH range from 80% to 90% in this setting.¹²⁻¹⁸ However, these assays have not yet been established to estimate the gene amplification status of these actionable/potential loci in OS.

For NGS analysis of bone tumors, in addition to sample aging, degradation of nucleic acids due to decalcification is a significant drawback of this analysis.¹ In addition, NGS analysis is very expensive (approximately \$4000 in Japan). Therefore, the establishment of a simple method is necessary. The findings obtained in this study were highly reproducible across many cancer cell lines, suggesting the reliability of our custom probe set. Furthermore, this NanoString-based CNV

assay using frozen samples revealed a mutually exclusive co-occurrence pattern of gene amplification in 3 of 13 cases (approximately 23%), which is still consistent with the previously reported frequency.¹ A quite recent study demonstrated a similar NanoString-based method for diagnosis of well-differentiated liposarcoma and dedifferentiated liposarcoma,¹⁹ however, CNV analysis by NanoString-based method to identify actionable targets leading to the molecular target therapy in OS has not been reported. Furthermore, the most notable point in this study is that almost the same findings were obtained in FFPE samples after decalcification with EDTA (83%), suggesting that the decalcification process, which often hampers NGS analysis, does not affect this analysis. Notably, this analysis is relatively cheap (\$300 per sample: tumor-derived and the corresponding normal tissue-derived DNA is required) with a short TAT. Therefore, this analysis will contribute to the design of a therapeutic strategy based on the genome profiling of OS.

We obtained several findings from this analysis regarding chemotherapeutic effects and gene amplification. We found enhanced amplification of *CCND3/VEGFA* in 2 cases after chemotherapy, which has not been previously reported as a chemotherapy-resistance-associated combination. Angiogenesis is very important in the progression of OS and there are many preclinical and developmental research of targeted anti-angiogenic therapy for OS such as monoclonal antibody to VEGF (bevacizumab), tyrosine kinase inhibitors (Sorafenib, Apatinib, Pazopanib, and Regorafenib) and human recombinant endostatin (Endostar).²⁰ In addition, a most recent study showed that *VEGFA* is expressed at high-level in myeloid cells and osteoclasts in OS.²¹ Therefore, the change in *VEGFA* amplification status after chemotherapy might come from myeloid cells and osteoclasts in OS samples, although we selected cellular area for this FFPE-CNV analysis. In addition, amplification status does not necessarily correlate with gene expression and protein expression, thus the confirmation of protein expression by *VEGFA* IHC would be also necessary. In addition, it has been shown that *CDK4* overexpression is a predictive biomarker for resistance to conventional chemotherapy in OS.²² In this study, among the 8 cases available for information on chemotherapeutic effects, 3 cases showed amplification of *CDK4/MDM2* in samples before and/or after chemotherapy. However, the chemotherapeutic effects were grades 1, 2, and 3, respectively, and there seemed to be no obvious relationship with the chemotherapeutic effects. Furthermore, we encountered 2 cases (Cases #1 and 2) of OS in which CNV status was concordant between frozen and FFPE samples, but not between FFPE biopsy samples before chemotherapy and FFPE samples after chemotherapy from the same patient. Both cases showed a lower chemotherapeutic effect (grade 1). These findings suggest that chemotherapy might affect CNV status, especially in genes associated with chemotherapeutic resistance. This change in the CNV profiles would be resulting from the population changes of tumor cells before and after chemotherapy. Furthermore, a recent single-cell transcriptome study in OS revealed that clinical OS samples contain many cell types with complexity of the

tumor microenvironment such as inflammation, cell proliferation, and cell metabolism.²³ These different cell types in OS showing different expression profiles might show distinctive responses to chemotherapy and lead to the different CNV profiles in OS samples after chemotherapy. Thus, this analysis would be useful for planning different therapeutic strategies for the treatment of patients with OS after chemotherapy.

A few limitations are raised in this study. First, the status of CNVs of cell lines analyzed by the NanoString analysis was compared to those described in the CCLE database to confirm whether similar results were obtained (Supplementary Figure S1). Although this comparison showed almost similar trends, the fold changes in CNVs were not described in the CCLE database. Second, we have not examined the subsequent gene expression and protein expression levels in OS samples as expected events followed by gene amplification. It would be better also to evaluate this correlation in order to establish the future substitution of this system by IHC, a more conveniently accessible method, although the purpose of this study is to establish a rapid and accurate screening system compared to NGS. Finally, this study has lower number of cases and is underpowered to show any statistical significance, thus is preliminary and needs further validation.

Conclusions

We propose a rapid screening system for molecular target therapy of OS. This system can overcome the DNA fragmentation problem caused by the decalcification process by EDTA. Furthermore, especially for tumors after chemotherapy with higher chemotherapeutic effects, CNV analysis using FFPE samples is recommended where the histological evaluation of viable tumor cells is possible, although our findings suggest that there was no obvious difference between frozen and FFPE samples in the CNV analysis using the NanoString system.

Acknowledgments

This work was carried out in part at the Intractable Disease Research Center, Juntendo University. The authors would like to thank Dr Yasunori Okada, Department of Pathophysiology for Locomotive and Neoplastic Diseases, Juntendo University Graduate School of Medicine, Tokyo, Japan for kindly providing cell lines.

Author's Contribution

Keita Sasa: Investigation, Methodology, Formal analysis, Data curation, Writing—original draft, Writing—review and editing. Tsuyoshi Saito: Conceptualization, Methodology, Formal analysis, Data curation, Funding acquisition, Writing—original draft, Writing—review and editing, Supervision, Project administration. Taisei Kurihara: Methodology, Formal analysis, Data curation, Funding acquisition, Writing—review and editing. Nobuhiko Hasegawa: Methodology, Formal analysis, Data curation, Writing—review and editing. Kei Sano: Methodology, Formal analysis, Data curation, Writing—review and editing. Daisuke Kubota: Resources, Methodology, Formal analysis, Data curation, Writing—review and editing. Keisuke Akaike:

Resources, Methodology, Formal analysis, Data curation, Funding acquisition, Writing—review and editing. Taketo Okubo: Resources, Methodology, Formal analysis, Data curation, Funding acquisition, Writing—review and editing. Takuo Hayashi: Methodology, Formal analysis, Data curation, Writing—review and editing. Tatsuya Takagi: Supervision, Resources, Data curation, Writing—review and editing. Muneaki Ishijima: Supervision, Data curation, Writing—review and editing. Yoshiyuki Suehara: Conceptualization, Methodology, Formal analysis, Data curation, Project administration, Funding acquisition, Writing—review and editing, Supervision.

Declaration of Conflicting Interests

The authors declared no potential conflicts of interest with respect to the research, authorship, and/or publication of this article.


Ethical Approval

This study was reviewed and approved by the Juntendo University School of Medicine Institutional Review Board (#21-079).

Funding

The authors disclosed receipt of the following financial support for the research, authorship, and/or publication of this article: This study was supported by a Grant-in-Aid from the Japan Society for the Promotion of Science (JSPS) KAKENHI (JSPS: grant numbers 19H03789 and 19K22694 to Y.S.; 19K16753 to K.A.; 18K15329 to T.O.; 20K22963 to T.K.; and 20K07415 17K08730 to T.S.).

ORCID iD

Tsuyoshi Saito  <https://orcid.org/0000-0001-9690-8440>

Supplemental Material

Supplemental material for this article is available online.

References

1. Suehara Y, Alex D, Bowman A, et al. Clinical genomic sequencing of pediatric and adult osteosarcoma reveals distinct molecular subsets with potentially targetable alterations. *Clin Cancer Res*. 2019;25(21):6346-6356. doi:10.1158/1078-0432.
2. Gill J, Gorlick R. Advancing therapy for osteosarcoma. *Nat Rev Clin Oncol*. 2021;18(10):609-624. doi:10.1038/s41571-021-00519-8.
3. Sayles LC, Breese MR, Koehne AL, et al. Genome-informed targeted therapy for osteosarcoma. *Cancer Discov*. 2019;9(1):46-63. doi:10.1158/2159-8290.CD-17-1152.
4. Zhao J, Dean DC, Hornicek FJ, Yu X, Duan Z. Emerging next-generation sequencing-based discoveries for targeted osteosarcoma therapy. *Cancer Lett*. 2020;474:158-167. doi:10.1016/j.canlet.2020.01.020.
5. Do H, Dobrovic A. Sequence artifacts in DNA from formalin-fixed tissues: causes and strategies for minimization. *Clin Chem*. 2015;61(1):64-71.
6. Hill NT, Kim D, Busam KJ, Chu EY, Green C, Brownell I. Distinct signatures of genomic copy number variants define subgroups of merkel cell carcinoma tumors. *Cancers (Basel)*. 2021;13(5):1134. doi:10.3390/cancers13051134.

7. Szatkiewicz JP, Fromer M, Nonneman RJ, et al. Characterization of single gene copy number variants in schizophrenia. *Biol Psychiatry*. 2020;87(8):736-744. doi:10.1016/j.biopsych.2019.09.023.
8. Meyers PA, Schwartz CL, Krailo M, et al. Osteosarcoma: a randomized, prospective trial of the addition of ifosfamide and/or muramyl tripeptide to cisplatin, doxorubicin, and high-dose methotrexate. *J Clin Oncol*. 2005;23(9):2004-2011. doi:10.1200/JCO.2005.06.031.
9. Liu W, Wang R, Zhang Y, et al. Whole-exome sequencing in osteosarcoma with distinct prognosis reveals disparate genetic heterogeneity. *Cancer Genet*. 2021;256-257:149-157. doi:10.1016/j.cancergen.2021.05.013.
10. Disel U, Madison R, Abhishek K, et al. The pan-cancer landscape of coamplification of the tyrosine kinases KIT, KDR, and PDGFRA. *Oncologist*. 2020;25(1):e39-e47. doi:10.1634/theoncologist.2018-0528.
11. Gupta S, Ito T, Alex D, et al. RUNX2 (6p21.1) amplification in osteosarcoma. *Hum Pathol*. 2019;94:23-28. doi:10.1016/j.humpath.2019.09.010.
12. Hofmann E, Seeboeck R, Jacobi N, et al. The combinatorial approach of laser-captured microdissection and reverse transcription quantitative polymerase chain reaction accurately determines HER2 status in breast cancer. *Biomark Res*. 2016;4:8. doi:10.1186/s40364-016-0062-7.
13. Perez EA, Cortes J, Gonzalez-Angulo AM, Bartlett JM. HER2 testing: current status and future directions. *Cancer Treat Rev*. 2014;40(2):276-284.
14. Bofin AM, Ytterhus B, Martin C, O'Leary JJ, Hagmar BM. Detection and quantitation of HER-2 gene amplification and protein expression in breast carcinoma. *Am J Clin Pathol*. 2004;122(1):110-119.
15. Portier BP, Wang Z, Downs-Kelly E, et al. Delay to formalin fixation 'cold ischemia time': effect on ERBB2 detection by in-situ hybridization and immunohistochemistry. *Mod Pathol*. 2013;26(1):1-9.
16. Ross JS, Fletcher JA, Bloom KJ, et al. HER-2/neu testing in breast cancer. *Am J Clin Pathol*. 2003;120(Suppl):S53-S71.
17. Dybdal N, Leiberman G, Anderson S, et al. Determination of HER2 gene amplification by fluorescence in situ hybridization and concordance with the clinical trials immunohistochemical assay in women with metastatic breast cancer evaluated for treatment with trastuzumab. *Breast Cancer Res Treat*. 2005;93(1):3-11.
18. Perez EA, Press MF, Dueck AC, et al. Immunohistochemistry and fluorescence in situ hybridization assessment of HER2 in clinical trials of adjuvant therapy for breast cancer (NCCTG N9831, BCIRG 006, and BCIRG 005). *Breast Cancer Res Treat*. 2013;138(1):99-108.
19. Wang XQ, Wang XQ, Hsu ATYW, Goytain A, Ng TLT, Nielsen TO. A rapid and cost-effective gene expression assay for the diagnosis of well-differentiated and dedifferentiated liposarcomas. *J Mol Diagn*. 2021;23(3):274-284. doi:10.1016/j.jmoldx.2020.11.011.
20. Liu Y, Huang N, Liao S, et al. Current research progress in targeted anti-angiogenesis therapy for osteosarcoma. *Cell Prolif*. 2021;54(9):e13102. Epub 2021 July 26. doi:10.1111/cpr.13102.
21. Feleke M, Feng W, Song D, et al. Single-cell RNA sequencing reveals differential expression of EGFL7 and VEGF in giant-cell tumor of bone and osteosarcoma. *Exp Biol Med*. 2022;247(14):1214-1227. doi:10.1177/15353702221088238.
22. Iwata S, Tatsumi Y, Yonemoto T, et al. CDK4 Overexpression is a predictive biomarker for resistance to conventional chemotherapy in patients with osteosarcoma. *Oncol Rep*. 2021;46(1):135. doi:10.3892/or.2021.8086.
23. Liu Y, Feng W, Dai Y, et al. Single-cell transcriptomics reveals the complexity of the tumor microenvironment of treatment-naïve osteosarcoma. *Front Oncol*. 2021;11:709210. doi:10.3389/fonc.2021.709210.